Fuzzy Controller Based Reserve Management in Hybrid Microgrid for Frequency Regulation

Phani kumar K.S.V, S. Venkateshwarlu

Abstract*: Power quality is a growing concern with sensible and critical loads asking for stringent frequency regulations. The distributed generation sources like Solar Photovoltaic, Diesel Generator, Fuel Cells, and Battery driven Electric Vehicles (BEV) are considered as power sources in the system. For the power-sharing among these generators, a central controller with a novel simple adaptive-additive control strategy is used. Each source has a local controller to regulate the power outputs. This paper presents a Neuro-Fuzzy controller for operating Solar Photovoltaic power at a Limited Power Point while a novel Neuro-Tuned-Fuzzy Controller decides which BEVs to be connected to the microgrid by giving a priority value to each BEV. The simulation results show the coordinated operation of the central and local controllers to regulate the power outputs of the sources was effective to manage reserves and achieve frequency regulation.

***Keywords*: Vehicle to Grid; Neuro Fuzzy Controller; Frequency Regulation; Energy management.**

I. INTRODUCTION

In the growing energy scenario, the development of the power structure has become essential. Microgrids are promising in supporting the conventional power system. The microgrid manages the distributed generation and the local loads with the constraints such as source availability [1]. It also takes care of critical loads and can support the main grid during load variations. It can be operated in two modes: 1. Grid-connected mode 2. Islanded (standalone) mode. In grid-connected mode, the peak load is shared by the microgrid thereby preventing utility grid failure. In standalone mode, the microgrid is isolated from the utility grid supporting the local loads connected to the microgrid. Because of the intermittent nature of the renewable sources, the distributed generation in microgrid must supply the varying loads with the constraint of variable energy availability. This creates a supply demand gap which results in frequency and voltage deviations in the microgrid. These deviations can cause severe damage to the loads connected and effect the system infrastructure. These problems are dominating in case of the islanded mode. In case of grid connected mode when the demand can't be fulfilled by the microgrid the utility grid can support the load and vice versa. Therefore, in an isolated microgrid, there is a necessity of a robust load frequency control (LFC) strategy which can suffice the active power requirements of the load and stabilize the voltage and frequency such that their deviations are under acceptable limits [2]-[4].

There is a major growth in electric vehicles (EV) and plug-in hybrid electric vehicle (PHEV) technologies due to stress on reduction of fuel usage and emission of greenhouse gases [5]. The charging of BEVs by connection to the microgrid varies the impedance and may require additional compensating elements in the circuit. Microgrid to vehicle charging can lead to issues like loss-of-power due to efficiency of converters, non-linear power drawn from microgrid, due to which power quality issues like harmonics and voltage imbalances, surges occur [5]. BEV User's demand to get fast charging will make the demand side management more complex since they become prime customers to the utility. One of the possible solutions is to make vehicle charging off-grid. Independent power producers (IPP) shall have solar based power source and sell the power to BEV owners, like the operation of a vehicle diesel/petrol filling station. The charging rates of vehicles can vary based on the geographical location being in metropolis / towns / highways etc. [6].

BEVs look like great substitute for Battery Energy Storage Systems (BESS) because of the energy saving and being environmentally friendly [7][8]. Almost entire day (95% of time) private electric vehicles remain idle in their parking. During this period, BEVs can be employed for frequency regulation. The load frequency controller helps in managing the real power variations in the system and maintaining the frequency within the desirable limits to improve the system performance [11]. Many researchers have utilized this vehicle-to-grid technology for the realization of LFC mechanism in an isolated microgrid [10]. With better load frequency control strategies, the energy efficiency, reliability, quality of power is improved the need for protective devices is reduced and therefore the overall maintenance cost of the system is reduced.

In this paper a microgrid is considered with a Diesel driven IC engine coupled with a synchronous generator, called a Diesel Generator as a source. A Fuel-cell is available with enough supplies of hydrogen and oxygen cylinders to send power to microgrid. A solar power plant is considered as another power source to utilize the renewable energy of solar insolation. The BEVs available at the parking lots are also considered for sharing the load power and participate in frequency regulation.

For sharing the load among these hybrid generation and to maintain system frequency, the traditional PI controllers and artificial intelligent techniques like fuzzy and neural networks have been used [12 13, 14] with the power generation constraints and system constraints like frequency limits.

Revised Manuscript Received October 05, 2019
***** Correspondence Author
Phani kumar K.S.V*, Electrical and Electronics department, CVR College of Engineering, Hyderabad, India.
S. Venkateshwarlu, Electrical and Electronics department, CVR College of Engineering, Hyderabad, India.

The novelty in this paper can be listed as:

(i) Introduction of plug-in and plug-outs of BEVs and studying the impact on frequency regulation.

(ii) Introducing dynamic load variations in small signal stability analysis.

(iii) Proposing a simple additive-adaptive-algorithm (AAA) to schedule power generation.

(iv) Proposing a Neuro Tuned Fuzzy Controller (NTFC) to manage the BEV fleet by prioritizing the vehicle to be connected to microgrid.

(v) Checking stability of frequency when solar insolation is changing.

The variations in load and deviation in power supplies are to be dealt-with using a central controller (with AAA) and decentralized local controllers like Proportional-integral (PI) and Neuro-fuzzy to maintain the frequency regulation in the system within the limits of ± 0.05Hz. MATLAB simulation is performed by modelling the sources and load. Results have been analyzed and presented by considering four scenarios and sub-cases where necessary. The schematic of the paper is as follows the system description is explained in detail in Section -II. The NTFC proposed for BEVs is described in Section III. the integrated operation of the system with methodology is explained in Section-IV. The simulation results and their analysis has been presented in section V. Conclusive statements with references are provided.

II. SYSTEM DESCRIPTION

The main objective is to maintain the frequency regulation between ± 0.05Hz. When there is a sudden change in load, the system frequency tends to change. In a traditional system with synchronous generators, there is inertia offered by the rotating parts, and hence the rate of change of frequency is controlled. With renewable power generators like Solar PhotoVoltaic (PV), Fuel Cell (FC), BEVs (charged by off-grid solar), the inertia must be provided by controlling the power output of these sources. In literature, [15] different methods to introduce inertia is discussed. In this paper, wind energy is not considered, since its availability is subjective to air velocities and installation area availability. Hence the kinetic energy stored in a wind turbine is not available to provide inertia. The other three methods are (a) operating the Solar PV at lower than optimum power points so that the output can be adjusted when load changes occur. (b) having an energy storage system and (c) having load side control. In this paper, all these methods are considered.

A solar power plant is considered with Limited Power Point Tracking (LPPT) method [16] designed using a Neuro fuzzy controller. The typical power output variation of a solar panel with the output terminal voltage (after modification using boost converters) is shown in Figure 1. The maximum power output is achieved when the voltage is Vm. When the generator operates at this point, and if load increases on the system, there is no scope for increasing the power output unless some other source is aiding (e.g. Battery). Suppose we operate at 90% of the PMAX, i.e. at P90%, and there is a power increase request, we can increase the power output by shifting the output voltage from V_1 or V_2 towards V_m. The slope of the graph on the left side of Vm is smaller than that on the right-hand side. For small changes in voltage, more power control is achieved on right hand side. This is desirable and hence point 'B' is selected to be the LPP instead of point 'A'. In case the load decreases, operating point B can be shifted further down, say point 'C' at a voltage of V_3. So, variation of voltage from V_m to V_3 can make the Solar PV react to frequency changes in the system. But as the temperature of the panel and insolation levels change, this graph also shifts. The points of V_m, V_2 are to be recollected for every possible value of temperature and power output required. Hence a neural network-based controller was designed to find the points Vm and V_2, while a fuzzy logic controller was designed to modify the reference value for voltage of the panel. [16]

A dedicated battery backup support is needed in a microgrid to supply electrical energy when the load escalates suddenly or during a generator outage, and to absorb the excess energy in the system when load levels fall instantaneously. This is a conventional method under use. But considering the investment cost and life of the battery, it is no longer a feasible solution to support frequency regulation [14]. There are batteries available in the MicroGrid with the owners of Electric Vehicles, who can charge their batteries with off-grid solar installations. On a full charge, given the probable utility of the vehicle for commute, [17-18] there is excess power in the battery that can support the microgrid for frequency regulation in a Vehicle to Microgrid mode (V2µG). In this paper two parking lots are considered each having a capacity to park five vehicles, preferably Cars. A fuzzy logic-based controller tuned by a neural network is proposed to manage the V2µG connections and is discussed in the next section.

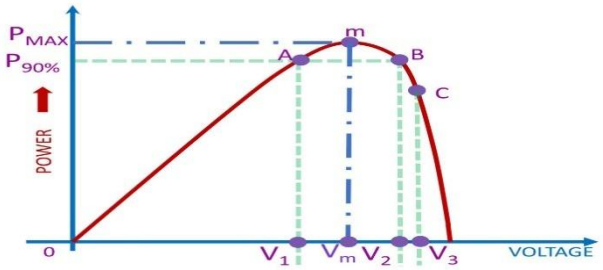

Fig. 1.Solar PV output power vs Voltage graph for LPPT

Power generation and load are normalized and represented in per-units (pu). Assuming that the system's maximum generation capacity is 1.21 pu, the peak demand is 1.24pu. To supply the excess 0.3 pu load, a reserve capacity is needed. In the system considered, solar and BEVs provide the reserve (spinning). But if the load increases beyond this value, there is only one option left to the microgrid-operator, to shed excess loads in the system. A microgrid is assumed to have critical loads and non-critical loads. Assuming that the grid operator has accessibility to control these loads individually, the non-critical loads are curtailed, to bring frequency under control. A typical system considered in the paper with four sources of generation is assumed to be distributed in the geographical area of the microgrid, with local controllers at their sites and a Central Controller (CC) at the grid-operator as represented in Figure 2 with necessary signal flows.

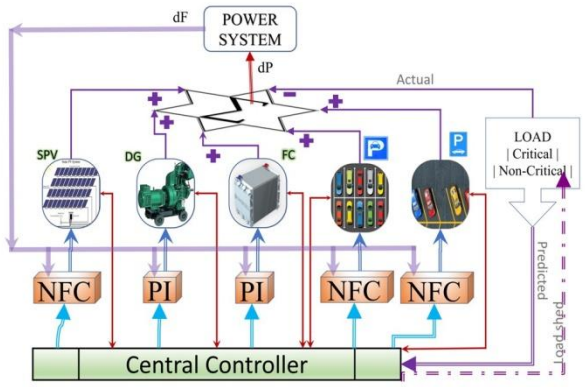

Fig. 2.Schematic of the microgrid considered in the paper

III. NEURO-FUZZY CONTROLLER FOR ELECTRIC VEHICLES

BEVs considered in the paper are assumed to be parked at two locations spread out in the geographical area of the microgrid, to place the generation site close to the load point. The availability of these vehicles at the parking lots is predicted [19]. It is understood that the BEVs come with varied State-of-Charges (SoC), battery capacities, plug-in timings and plug-out times. So, it becomes important for this Independent Power Producer (Parking lots) to make sure that a reliable and continuous power supply is given to the microgrid. Owner of the vehicle will impose a constraint that the battery SoC should not decrease below a given value since the vehicle has to be driven for a certain distance before the battery is kept on charge. This is called $SoC_{k,min}$, where 'k' is the vehicle number.

$$S(k) = \begin{cases} 1 \ if \ SoC_k > SoC_{k,min} \\ 0 \ if \ SoC_k \leq SoC_{k,min} \end{cases} \quad (1)$$

The operator/controller must choose the best possible combination of BEVs based on the parameters mentioned above. The following decisions are obvious to an Independent Power Producer (IPP) operator: (a) when discharge rates are higher or lower, preference for batteries with medium SoC is high. This is to retain the batteries with higher SoCs for longer time ranges. This also enhances reliability and reserve capacity of the system. (b) when a BEV's SoC is less than 20%, irrespective of the system conditions, the priority is kept low to zero, since the life of the battery is at stake. In order not to encourage the battery charging beyond 90%, as the battery health is affected, the priority levels are reduced.

The task is to incorporate these characteristics into the controller. Traditional and learning based approaches are being applied in the controllers to deal with the energy management [20]. For each BEV, there are two variables to deal with. One is the state of charge of the battery 'k' SoCk, and the other is Discharge-rate (Dr). To start with, a two-variable function, f(SoC, Dr), has been designed using Fourier Series as shown in the equation 2. The parameters in the equation of tuned in such a way that the expected characteristics are achieved to the maximum possible extent. Batteries with SoC values from [0 40] have an approximate linear positive slope in the priority value. From [40 60], the priority value is almost the same, while from [60 90] the priority increases but from [90 100]%, the priority decreases again. A 3D graphical representation has been shown with is SoC on the x-axis the discharge rate on the y-axis and priorities order on the Z axis.

$$Dr_k(j) = a_{0,k} + \sum_{i=1}^{2} a_{i,k} \cos\left(i * w * SoC_{j,k}\right) + bi,k\sin i*w*SoCj,k \quad (2)$$

Where $Dr_k(j)$ is the value of Dr for k∈ [0 1] and for j ∈ [0 100]. a_0 is a constant, a_i, b_i are coefficients, w is the weightage factor. The coefficient values for k = 0.5 are given as $a_{1,0.5}$ = -15.48, $b_{1,0.5}$ =-26.39, $a_{2,0.5}$ = -13.45, $b_{2,0.5}$ =-10.18, a0 = 48.53, and w = 0.05048;

Sum-of-Sine based equation is also found to be suitable to express the behavior of the controller to an extent. The Equation 3 shows the basic formula used in the paper for this approach. The parameters of the equation are tuned optimally to achieve the expected characteristics. The graphical representation of the equation with SoC values varying from [0 100] percentage and the discharge rate values varying from [0 1] is presented in the Figure 3 (c), (d).

$$Dr_k(j) = \sum_{i=1}^{3} a_{i,k} \sin\left(b_{i,k} * SoC_j + c_{i,k}\right) \quad (3)$$

Where $Dr_k(j)$ is the value of Dr for k∈ [0 1] and for j ∈ [0 100]. $a_{i,k}, b_{i,k}, c_{i,k}$ are the coefficients specific for a 'k' value where i = 1,2,3. The typical values for k = 0.5 are given as $a_{1,0.5}$ =124.6, $b_{1,0.5}$ =0.04463, $c_{1,0.5}$ = -0.7867, $a_{2,0.5}$ =445.8, $b_{2,0.5}$ =0.07432, $c_{2,0.5}$ =147, $a_{3,0.5}$ =380.5, $b_{3,0.5}$ =0.07834, $c_{3,0.5}$ = 4.441.

These two equations do not satisfy the overall requirement and hence there is a necessity to design a controller which can merge the characteristics of these two equations together. A learning-based approach can be used such as a Fuzzy Logic controller or using a neural network-based controller. On computational basis a neural network-based controller shall take more time than a Fuzzy Logic controller [21]. Another option is to utilize the advantages of neural network to train for design the parameters of a Fuzzy Logic controller so that the intelligence of a neural network can be embedded into a Fuzzy Logic controller.

For training the neural network the data available from these two equations with some modifications is taken into consideration and further fine-tuned so that the desirable characteristics are achieved. A total of 10,000 samples were taken, out of which 75% are used to tune the parameters, 15% of the data is used to test the network and the remaining 10% for validation. A typical 2 input one output model with one hidden layer is chosen as the architecture with three trapezoidal membership functions considered for two input variables and the output variable. The final surface view of the fuzzy logic controller output is presented in Figure 3(e) and 3(f).

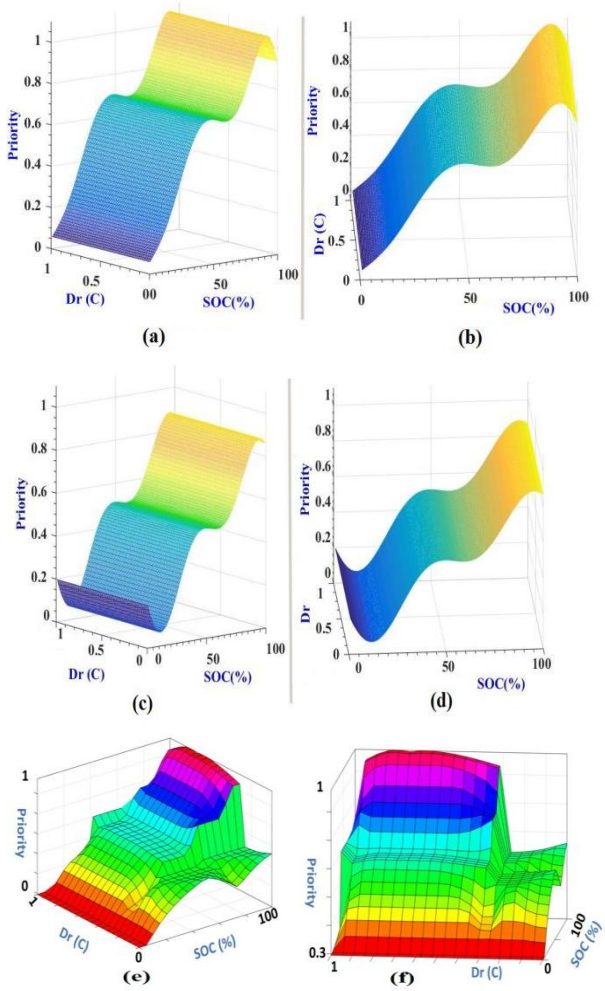

Fig. 3.Priority based on (a,b) Fourier Series (c,d) Sum-of-Sines (e,f) Neuro-trained Fuzzy Logic controllers

To show the effectiveness of the Fuzzy Logic controller designed difference between the responses of the controllers is analyzed by applying different discharge rates as the SoC is changing from [0 100] percentage. Figure 4 shows difference in the values of output obtained from the NTFC and the sum-of-sines based controller for different Dr values. while Figure 5 shows difference in the values of output obtained from the NTFC and the Fourier Series based controller for different Dr values. These graphs indicate that for the SoC values in the range [30 40] % and [80 90] %, there is a significant difference in the output values ranging from -0.3 to + 0.3.

If NTFC's output is taken as reference, from Figure 4(a), it can be observed that the error approaches '0' for medium range SoCs and then stays intact for higher Drs, as the SoC levels are increasing. But for lower SoC values the error rates are quite significant. While in Figure 4(b), there is a relatively less deviation from the NTFC controller for mid-range SoCs, compared to the error shown in Figure 4. The Root-Mean-Square-Error of these errors is around 0.1474 for equation 2 and 0.1613 for equation 3, which is quite significant. Since these two equation-based controllers do not implement the exact rules, NTFC is chosen to manage the V2μG in the parking station so that depending on the grid's requirement, BEVs can send the power to the grid. Remaining vehicles will be considered as a spinning reserve.

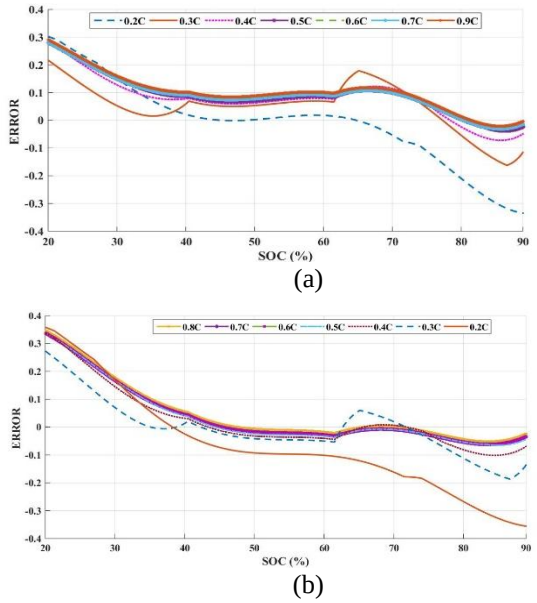

Fig. 4.Difference between responses of controllers based on (a) Sum of Sines (SoS) and NTFC. (b) Fourier Series and NTFC.

IV. METHODOLOGY

Integrated operation of the power generating sources for improved frequency regulation is to be obtained in a system having LC at the generation site and CC at the microgrid operator. CC schedules the power generation based on the load data available. A series of step changes is considered as the load data, called the predicted load. Scenarios are considered in the paper with a modified load signal, called 'actual load' being sent to the power system. The microgrid is also tested for its adaptiveness to the difference between the predicted and actual loads. The CC follows a simple additive-adaptive based algorithm to identify the power generation set-values and sends them to the local controllers available at the generator sites. A complex unit commitment-based solution is not necessary, because the priorities of the generators are prefixed. The ranking order is shown in Figure 6. Feedback is taken whether there is any deviation of the actual power generated by the source to the set-value. This difference may arise due to the dF command received by LCs from the power system. The details regarding designing of LCs for sources can be referred to [16]. Feedback obtained from the generators is then checked for constraints (maximum and minimum generation). If any violation occurs, the corresponding set-values are reduced and the generator in the next priority list must take up that load. If all the generators are delivering power at their maximum set points (except solar PV), then the reserve capacity can be added to the microgrid power. Availability status of BEV_k is decided based on whether (a) BEV_k is plugged in (b) BEV_k is plugged out and (c) the SoC limits are under the limits set by the user. The status can either be '0' or '1'. In this paper NTFC is used for prioritization of BEV participation in the grid, as mentioned in the previous section. The outputs of each NTFC is gathered by an operator and then cross checked for its availability. Only if the BEV is available, its priority value is stacked for that time 't'.

Otherwise that BEV is not considered for participation. Once the final stack of priorities is available along with the respective BEV identification number, sorting is done in descending order and the vehicles with top priorities are connected to the microgrid when required.

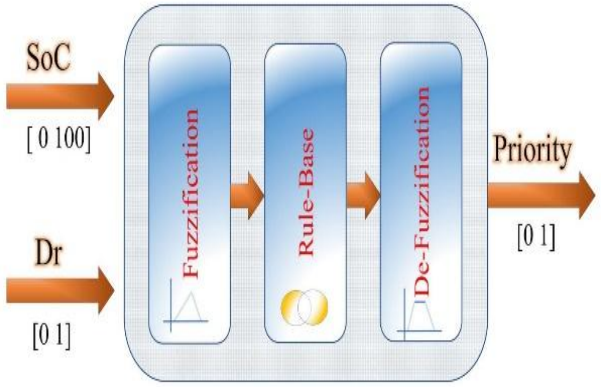

Fig. 5.Schematic of NTFC for BEV prioritization

Fig. 6.Algorithm for commitment of load used by CC.

CC sends a power requirement set-value command to each parking-lot operator. The operator shall allocate high priority BEVs until the set value is reached. The discharge rate shall be common for each battery irrespective of its capacity. Care is taken to limit the discharge rates so that the lowest capacity battery is not affected.

V. SIMULATION RESULTS AND ANALYSIS

In this paper four scenarios are considered. In the first scenario, NTFC controller designed for the parking lot is tested during small signal stability analysis performed on the system (to analyze frequency regulation). In the next scenario, solar insolation is varied, and Solar PV output is controlled by its Neuro-Fuzzy controller. The integrated operation is tested for its ability to regulate frequency. Scenario-3 deals with dynamic load variations (small and continuous) in addition to the transients (step changes), to simulate a real time load change. Extreme load conditions are imposed on the system and the system response is analyzed in the fourth scenario. Certain assumptions are made before simulating the system. They are (a) DG is available with necessary diesel reserves. (ii) FC has enough supply of hydrogen and oxygen reserves (iii) Solar insolation is available throughout the simulation time. (iv) Critical load considered in the system is 0.2 pu. (iv) BEVs are charged from off-grid solar power. (v) Microgrid operator nor the IPP operator are interested in profits. (vi) BEVs parking at parking-lot-1 are numbered 1 to 5. while BEVs parking at parking-lot-2 are numbered 6 to 10. The minimum and maximum generation capacities (pu) of the sources considered are shown in the Table 1.

Table- I: Minimum and maximum generation capacities (pu) of the sources

Source	Diesel	Fuel Cells	Solar PV	Sum of BEVs	Total
Min (pu)	0.1	0.1	0	0	0.2
Max (pu)	0.3	0.3	0.29	0.3 (@0.9C)	1.19
	dF signal response margin = +1.6%				1.21

A. Scenario-1 - With BEV parking lots

Three cases are considered in this scenario. BEV participation is randomly chosen for testing the NTFC's ability to select the best BEVs based on the discharge power signal from CC and SoC of the batteries. The initial battery SoCs of Electric Vehicles will be considered as shown in Table 2.

The load considered, shown in Figure 7, shall be common for the three cases under study in this scenario. For the initial 120s, the load remains same and thereafter for every 60s, a step load change is considered. 0s to 30s is the usual time taken by the system to respond steadily and the response during this period may be neglected.

Table II: SoC levels of the Batteries in Electric Vehicles at the beginning of simulation

	Parking Lot – 1					Parking Lot - 2				
BEV No	1	2	3	4	5	6	7	8	9	10
SoC (%)	89	75	60	90	40	74	87	78	81	87

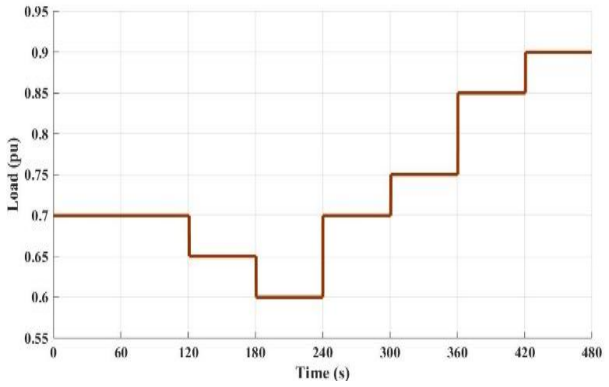

Fig. 7.Load pattern considered with step changes

1) Case - 1:

Considering all the BEVs are available for supplying power during the entire simulation period, the system is simulated for 480 sec and the results are analyzed in this case. Considering the load of 0.7pu at 0thsec, according to step 1 in Figure 6, DG is given set-value of 0.1 pu and FC is set to 0.1pu. Then Solar PV could generate 0.241 pu. The remaining load is 0.259pu. This is less than the maximum power generation capacity of parking lots together. Hence 0.259pu of the remaining load is supplied by the BEVs. Selection of the BEVs is based on the NTFC's output decision of priority value.

The priority value of each BEV in parking-lot-1 is shown in Figure 8 (a & b). Power sharing of the BEVs present in parking lots 1 and 2 is shown in figures 9 (a & b) respectively. Selection of these BEVs is based on the NTFC's output decision of priority value. From 0 to 360th sec, the discharge rate has not been so high and hence, the BEVs with high SOCs were connected to the microgrid.

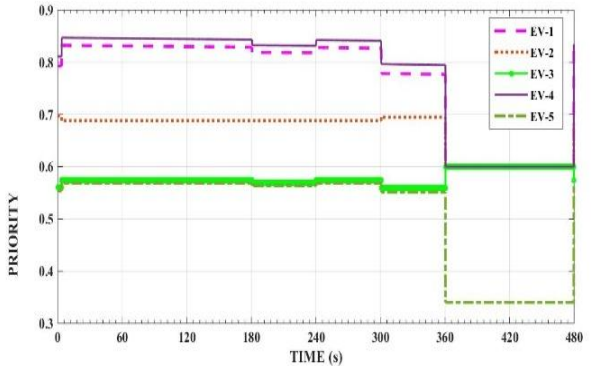

(a)

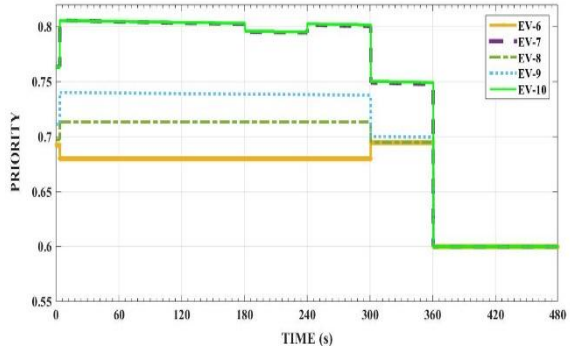

(b)

Fig. 8.NTFC's output priority levels for BEVs based on SoC and Dr (a) Parking-Lot-1 (b) Parking-Lot-2

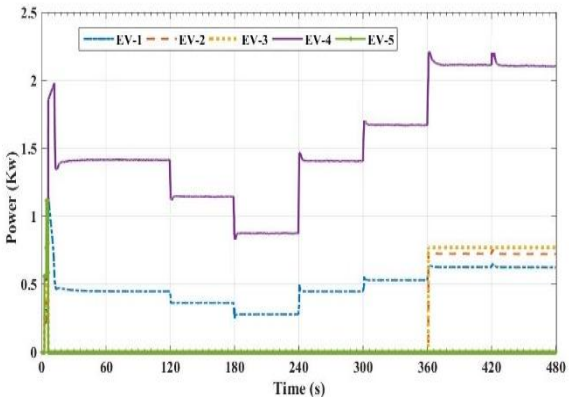

(a)

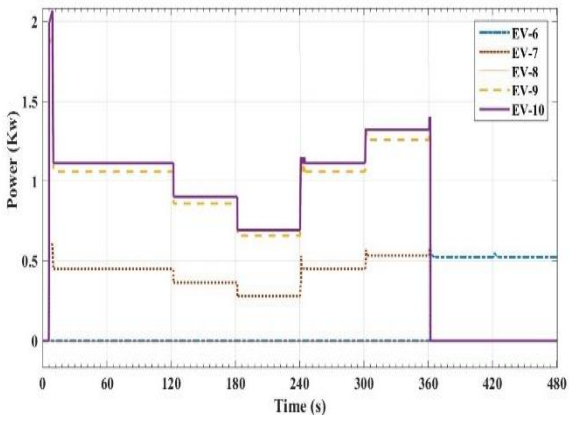

(b)

Fig. 9.Power generation of BEVs based (a) for Parking-lot-1 (b) for Parking-lot-2

After 360th sec, the load is high enough to extract maximum power capable from the parking-lots. Since the discharge rates are high, the priority values with medium SoC levels has been selected for microgrid connection. The overall power generation by the distributed resources is shown in the Figure 10. As the Power set value to the BEVs is increasing, the discharge rate will increase proportionately. The maximum capacity by the parking lot is also decided by the power handling capability of the cable and other associated elements of the circuit. During 0 to 360 seconds, BEVs 1,5,7,9,10 are supplying power as the discharge rate required is less and the SoCs of the batteries are high. After 360th sec, BEVs has reached maximum allowable power generation capacity, and hence FC has taken the additional load share. Solar PV is generating 0.241pu and DG 0.1pu throughout the simulation period of 480 seconds. At 360th sec, load value has changed from 0.75pu to 0.85pu and this brings sum of BEV power to its maximum. Now according to step 5, FC shall supply the additional load, but the response takes some settling time. Due to the mismatch between power generation and load, there is dF in the system. This dF signal is given to all the generators including BEVs. So, there is some additional power delivered beyond their maximum limits for a very short duration of time, not affecting the system's stability. This is the integrated operation of the sources to maintain the frequency regulation using the hierarchical control system

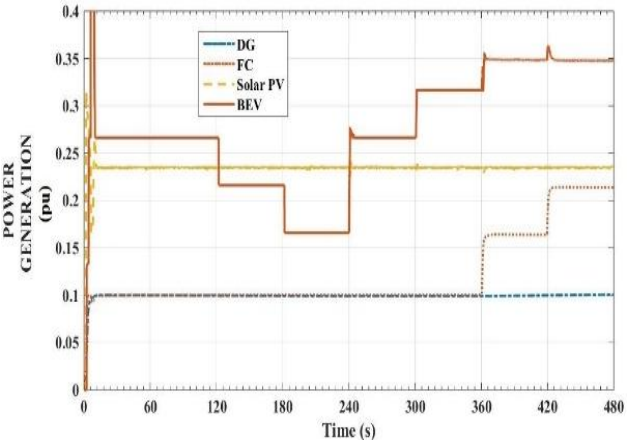

Fig. 10. PU power generation response from different sources

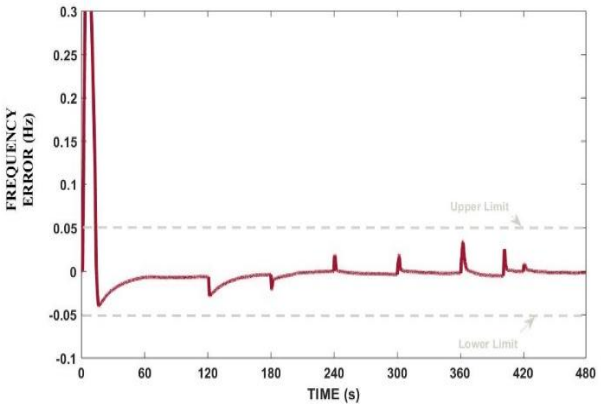

Fig. 11. Frequency error response of the system

Table 3: BEV Plug-in and Plug-out times in seconds

BEV-NO	1	2	3	4	5
Plug-In	20	60	0	0	0
Plug-Out	480	360	480	180	480

BEV-No	6	7	8	9	10
Plug-In	40	67	0	220	0
Plug-Out	480	400	480	300	480

The frequency error is observed to be within the limits and pushing towards zero point. Under higher discharge rates, the BEVs with medium SoC levels are preferred. Hence BEVs 1,2,3,4,6 are having more priority value and the load is being shared by these BEVs. Other BEVs are assumed to be in reserve mode. If any BEV must be disconnected because of less SoC, these batteries can be utilized

2) Case - 2: Considering Plug-in and Plug-out Times

The BEVs coming to the parking-lots need not necessarily be connected to the grid. In this context, a random selection of plug-in and plug-out times have been chosen as shown in Table 3. According to the algorithm given in Figure 6, after completion of step 3, the next step is to prioritize the BEVs based on their SoC and Dr. It is to be noted that every BEV's SoC is tracked by the operator since it is a continuous process of evaluation to yield precise data. This also helps the operator in extending the vehicle's utilization further. Hence, the information of all SoCs is available and CC gives the information of Dr. Hence parking-lot operators find the priority value of all BEVs. If a given BEV is not plugged-in, then its status is marked '0' and it shall not be committed. Figure 12 shows the priority levels of BEVs parking-lots 1 and 2. As stated earlier, the load profile remains the same. Similar to the previous case, the priorities change significantly after 360th sec since the load has increased beyond 0.81pu.

Few important observations from these figures are given here and further analysis is left to the reader. In the plug-in pattern, BEV-1 was coming-in at time t=20s with a priority value of 0.832, because of its higher SoC, so at time t=21s, it is immediately brought into service replacing BEV-5 having a priority value of 0.568. Similarly, BEV-6 was plugged-in at t=40s with a priority of 0.679 replacing BEV-3 which has a priority of 0.573.

At time t=60s BEV-2 has plugged-in with a priority level of 0.688 replacing BEV-6 which then had a priority level of 0.677. But at t=67s, BEV-7 took over BEV-2 with a priority difference of 0.117. It is to be noted that, once a BEV is connected to the microgrid, its SoC starts decreasing and hence the priority value also changes accordingly

. Few important observations from these figures are given here and further analysis is left to the reader. In the plug-in pattern, BEV-1 was coming-in at time t=20s with a priority value of 0.832, because of its higher SoC, so at time t=21s, it is immediately brought into service replacing BEV-5 having a priority value of 0.568. Similarly, BEV-6 was plugged-in at t=40s with a priority of 0.679 replacing BEV-3 which has a priority of 0.573. At time t=60s BEV-2 has plugged-in with a priority level of 0.688 replacing BEV-6 which then had a priority level of 0.677. But at t=67s, BEV-7 took over BEV-2 with a priority difference of 0.117.

It is to be noted that, once a BEV is connected to the microgrid, its SoC starts decreasing and hence the priority value also changes accordingly. The overall power generation by the sources in the microgrid is shown in Figure 14. This is similar to Figure 10 in case-1 with only difference in small surges of BEV output, trying to compensate the FC's slow time response and BEV-7's plug-off at t =400s.The frequency error graph is shown in Figure 15. Small surge values can be observed when load is having a step change but are within the boundary limits. Overall analysis shows that frequency regulation has been within the permissible limits.

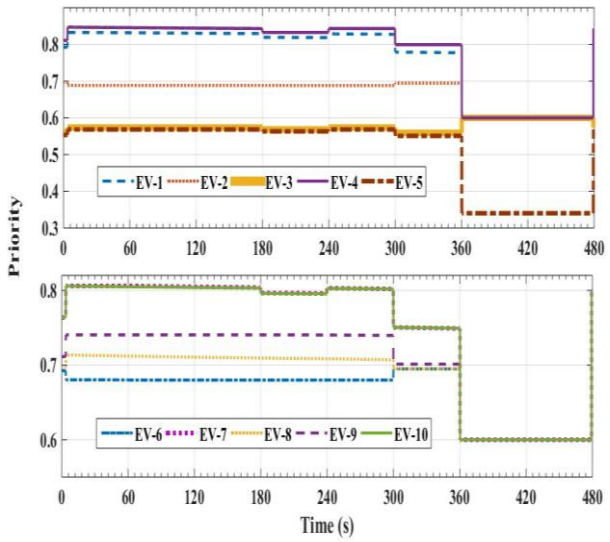

Fig. 12. Priority levels of each BEV at parking-lot-1 and 2 calculated by NTFC.

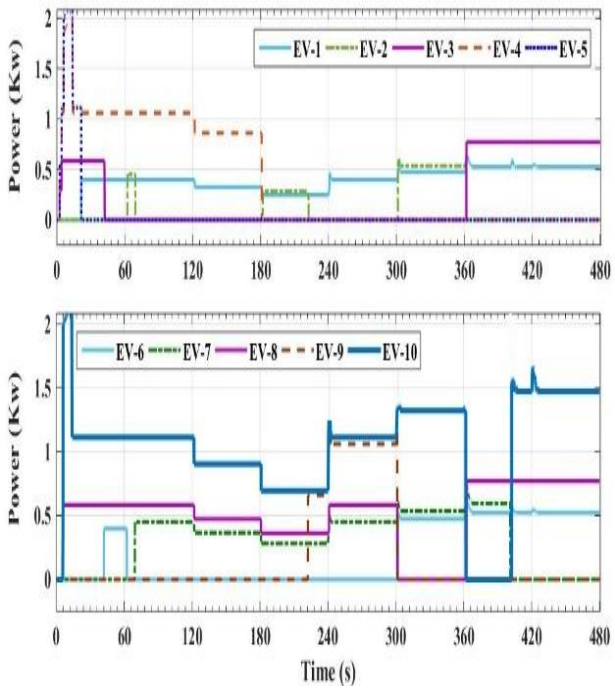

Fig. 13. Power production of each BEV at the parking lots 1 and 2.

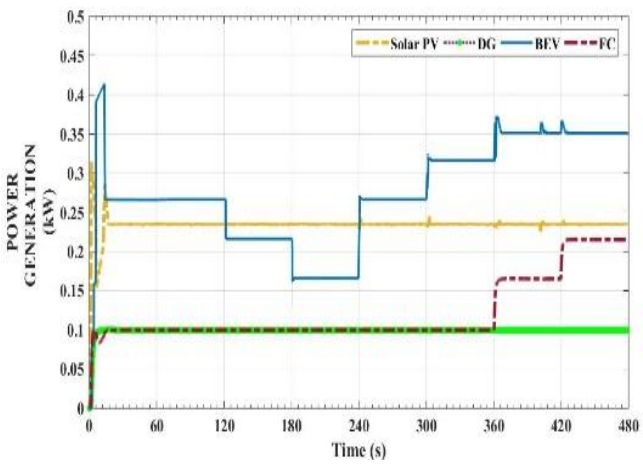

Fig. 14. Power generation response from different sources

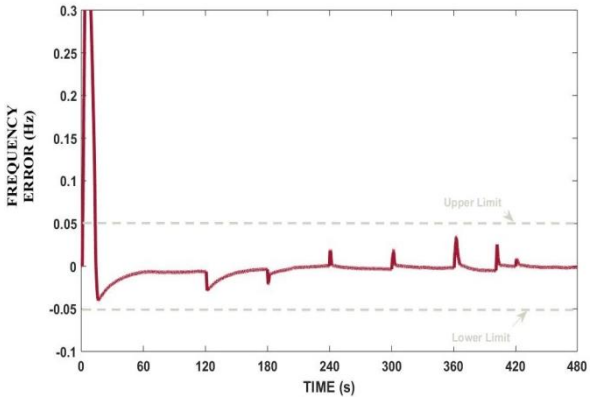

Fig. 15. Frequency error response of the system

3) Case - 3:

In this case the battery driven electric vehicle plug-in and plug-out data considered, as given in Table 4 is modified with more excursions by BEVs. Vehicles 6 and 9 are hardly available at the parking lots. Four other electric vehicles login at time t>0 and three electric vehicles opted to plug-out before the end of 480 seconds. The SoCs of these vehicles are according to table 2. As mentioned before, the priority levels of these vehicles depend on the current SoC values. The priority levels of these vehicles throughout the simulation time as shown in Figure 16. The power generation done by these BEVs is shown in Figure 17. It can be observed that electric vehicles 6 and 9 not supplying any power since they are not available in the parking lot. With electric vehicles 1 and 2 plugging in at 20 seconds and 60 seconds with high priority values, they become an obvious choice to be connected to the microgrid. After 360 seconds, when the load is increased priority levels of medium range SoCs of BEVs become more prioritized.

The power generated by all the sources considered in the micro grid is shown in Figure 18. This figure is similar to the previous case assuming that the power electronic switching of a BEV is fast enough to cause power surge of minimum magnitude. The impact of the surges can be seen in this figure compared to Figure 14. The frequency error obtained in this case is shown in Figure 19. Due to the changes in load and behavior of electric vehicles there are some deviations in the frequency response but are limited to the standards set by NERC [22].

Table 4: BEV Plug-in and Plug-out data times in seconds

BEV-No	1	2	3	4	5
Plug-in	20	60	0	0	70
Plug-out	480	360	480	180	480

BEV-No	6	7	8	9	10

Plug-in	0	67	0	0	0
Plug-out	0	400	480	40	480

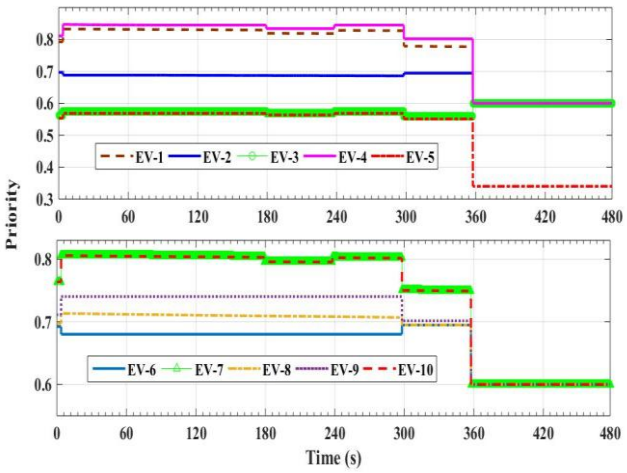

Fig. 16. Priority levels of BEVs

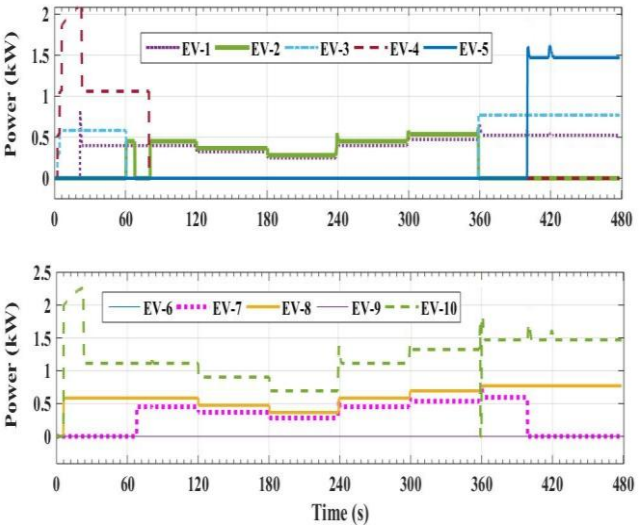

Fig. 17. Power generation response by individual BEVs

B. *Scenario-2 - With Variations in Load Pattern*

The load on power system is not constant, given the dynamic behavior of power consumption by loads such as lifts, escalators, Inverter ACs, automatic lighting system and Manual operation of loads. Performing small signal stability on constant characteristic of load until the step change will not give the complete stability picture of the system and particularly the frequency.

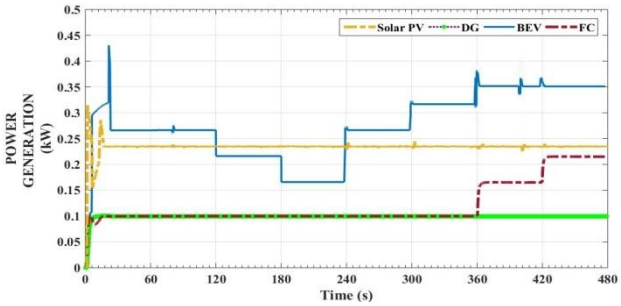

Fig. 18. Power generation by the sources in microgrid

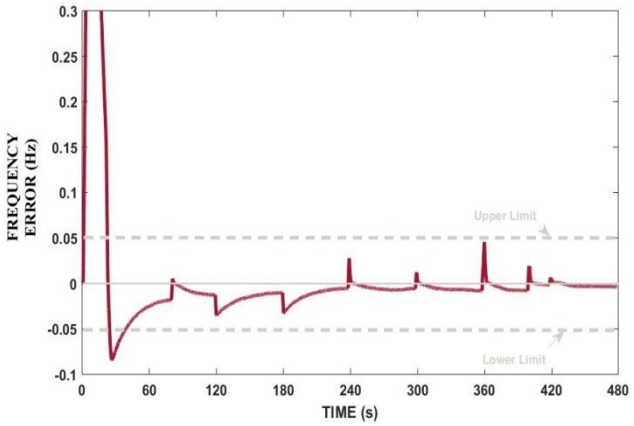

Fig. 19. Frequency error (dF) response of the microgrid power system

The frequency response of the system with small, continuous, non-periodic, dynamic load changes is considered in this scenario with step changes. The load profile is shown in Figure 20. The controller at the generation sites are not allowed to settle into a steady state and should deal with rapid variations in the rate of change of power (dP) and rate of change of dP ((dP)′). Solar PV is exempted from responding to variations, unless it is the last choice available, as sudden changes in inductor currents of the boost converter is practically not feasible and the reserve capacity cannot be maintained for peak loads.

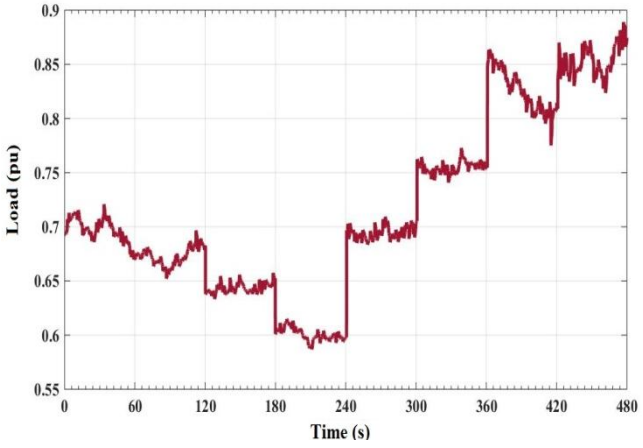

Fig. 20. Load profile considered in this Scenario

As the load is changing, the discharge rate (for parking lots) value also changes modifying the priority value rapidly. The controllers used have been efficient in dealing with changing priorities and step load changes. It can also be noted that BEVS are playing a vital role in adjusting to the load variations from 0 to 360 seconds. At 360th sec, due to load change from 0.75pu to 0.85pu, BEVs have reached maximum generation capability and hence FC takes additional load. The power generation by different sources is given in Figure 21. The response of FC to the dynamic load changes is slow and affecting the stability of frequency, but the error is well within the limits. The frequency response is plotted in Figure 22.

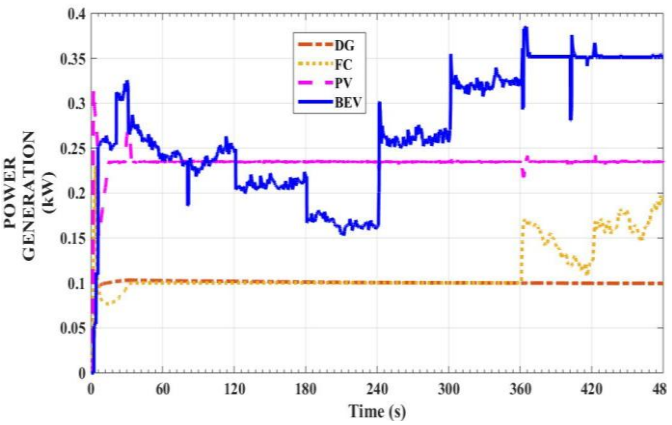

Fig. 21. Power Generation by all the sources committed

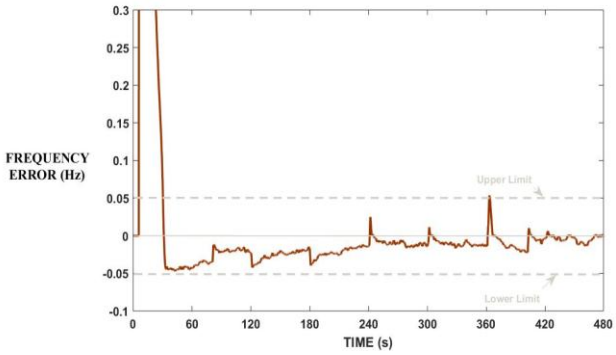

Fig. 22. Frequency Error response of the system

C. Scenario-3: *With Variations in Solar Insolation*

If solar insolation changes, the power output of the Solar PV varies (directly proportional), affecting the overall power sharing and reserve availability in the system. The parameters considered in the previous cases are continued here to increase the complexity of the system, like the plugin and plug out times from Scenario-1 Case 3. The insolation step changes considered in the paper is shown in Figure 23. For the load profile considered in scenario 2 case 1 (Figure 20), the power sharing by the sources is shown in the Figure 24. At 240th sec there is a step load change from 0.6pu to 0.7pu. Solar PV is generating at 0.14pu at an insolation of 300 W/m2. The remaining load is close to the maximum value of BEV generation (i.e. 0.35pu). Hence the BEV generation is committed accordingly. At 300th sec there is a step load increase and increase in insolation occurring simultaneously. The system is tested for its stability when the load and source are having disturbances.

Figure 24 reflects the power increase of Solar PV and FC taking share of the additional load. Due to plugging out of BEVs at 360th sec & 400th sec and replacement by other BEVs, there are surges in the power sharing because of the slow response from FC and dynamic load changes.

The overall frequency response is plotted in Figure 25. It can be observed that as the complexity of the system parameters are increasing, the fluctuations in the frequency error is also increasing, but the controllers at the generators are able to adjust the outputs to maintain frequency regulation.

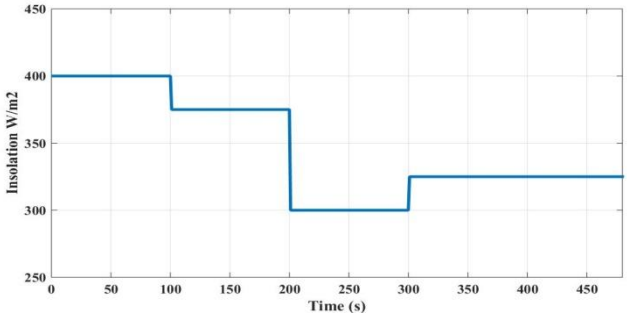

Fig. 23. Step Insolation changes considered in the paper

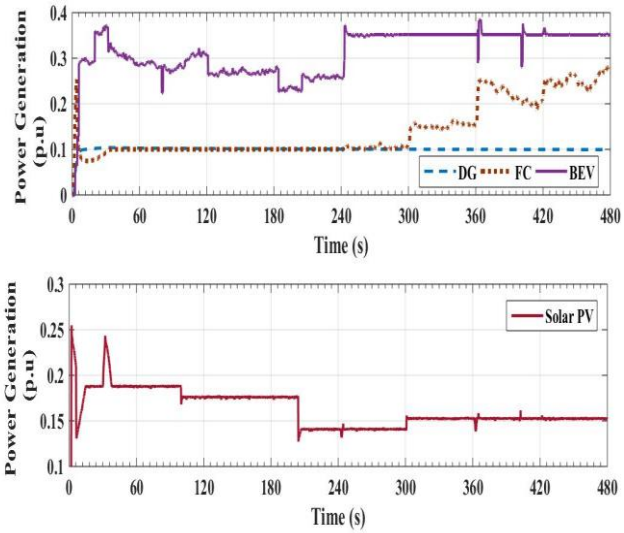

Fig. 24. Power Generation by various sources participating and by Solar PV

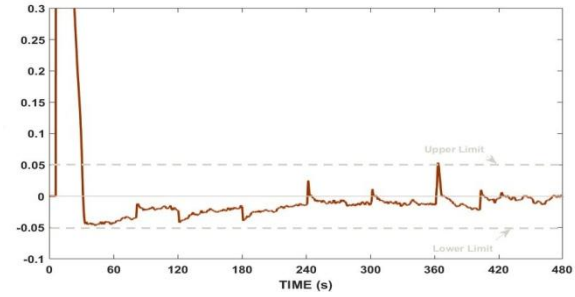

Fig. 25. Frequency regulation response of the microgrid system

D. Scenario-4 - Extreme Load Conditions

In the past three scenarios the range of load variation has been from around 0.594pu to 0. 892pu.This has not been a burden to the power sources since their maximum generation capability is 1.21pu. In this scenario we consider the variation of load from 1pu to 1.3 pu. The load profile being considered is shown in Figure 26. The parameters of BEVs considered in scenario 1 case 3 are applied here, while load signal is considered without white Gaussian noise and the Solar insolation variation is also not considered. At time t =0, the load is 1.1 pu. According to step 3 in the algorithm, DG is allocated 0.1pu and FC is given 0.1 pu share. Solar PV is generating 0.241pu power at LPP. The remaining load is

0.659pu. BEVs should now deliver their maximum power that is 0.35pu to the microgrid. Now the load to be scheduled is 0.301pu. Hence FC is now committed with more 0.2 per unit to reach its maximum capacity of 0.3pu. The remaining load is 0.109pu. Hence DG is now required to supply a total of 0.209pu. The BEV power sharing in parking lots 1 and 2 is shown in Figure 27. The Power generation by various sources in the system is shown in Figure 28.

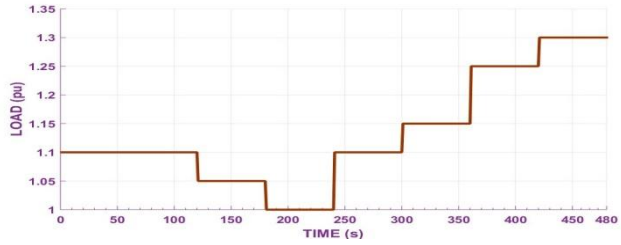

Fig. 26. Load profile considered for Scenario-4

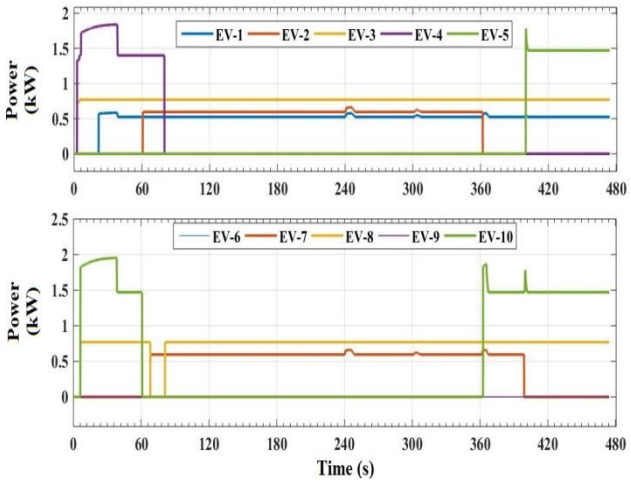

Fig. 27. BEV power sharing in parking lots 1 and 2

At 120th sec and 180th sec, when there is a step decrease in the load, DG is given first preference to decrease its power generation since the cost of generation is higher and the diesel resources must be preserved for supplying the base loads/critical loads of the system. At 240th sec, when there is a load change of 1pu to 1.1pu, the response of DG is slow and hence the frequency error signal is generated as shown in Figure 29. To compensate this FC has increased its generation beyond its rated maximum for short duration of time. When there is a load change from 1.15pu to 1.25pu the system's maximum generation limit of 1.21pu has been exceeded and the reserve capacity from solar PV is pumped into the microgrid.

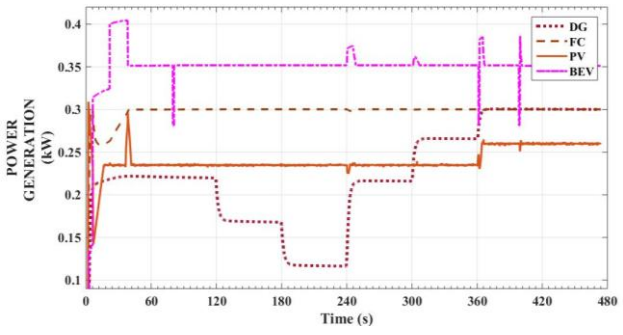

Fig. 28. Power generation by various sources in the system under extreme load conditions

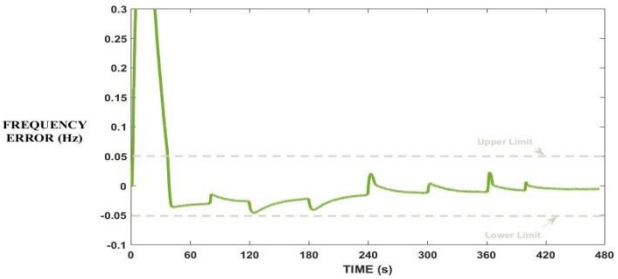

Fig. 29. Frequency response of the system to extreme load conditions

VI. CONCLUSIONS

Frequency regulation in a hybrid microgrid along with reserve management has been achieved with renewable power generating sources like Solar PV, DG, FC and BEVs. The integrated operation of the distributed resources with BEVs management has been demonstrated in the paper with simple adaptive-additive algorithm. The reserve management has been achieved without the help of a dedicated battery storage, by using a neuro-fuzzy controller for Solar PV and a neuro-trained-fuzzy controller for BEVs. For the first time the transient and dynamic behavior of the load and the power sources has been imposed on the microgrid scenario simultaneously and the proposed scheme has given excellent frequency regulation.

REFERENCES

1. Zhirong Xu, Ping Yang, Analysis on the organization and Development of multi-microgrids, Renewable and Sustainable energy reviews, Vol. 81, No. 2, 2204-2216, 2016.
2. P.S. R Murty, Electrical Power systems, Elsevier Ltd. United Kingdom, 2017.
3. S. Suryanarayanan and E. Kyriakides, Microgrids: An emerging technology to enhance power system reliability, IEEE Trans. Smart Grid, March 2017.
4. H. Jiayi, J. Chuanwen, and X. Rong, A review on distributed energy resources and MicroGrid, Renew. Sustain. Energy Rev, vol. 12, 2472–2483, 2008.
5. M. Ehsani, Y. Gao, S. E. Gay, and A. Emadi, Modern Electric, Hybrid Electric, and Fuel Cell Vehicles. Boca Raton, FL: CRC Press, 2005.
6. Shahid hussain, Mohamed a.ahmed and Young-chon kim, Efficient Power Management Algorithm Based on Fuzzy Logic Inference for Electric Vehicles Parking Lot IEEE Access, Volume 7 , 65467 – 65485, 2019
7. Manoj Datta, Tomonobuoj Senjyu, Fuzzy control of distributed PV inverters/energy storage systems/electric vehicles for frequency regulation in a large power system, IEEE Trans. Smart Grid, Vol. 4, No. 1, 479–488, 2013.
8. Willett Kempton, Jasna Tomi´ c, Vehicle-to-grid power implementation: from stabilizing the grid to supporting large scale renewable energy, Journal of Power Sources, Vol. 144, No.1, 280–294, 2005.
9. Leonardo E. Bremermann, Manuel Matos, Joao A. Pec¸ as Lopes, Mauro Rosa, Electric vehicle models for evaluating the security of supply, Electric Power System Research, Vol. 111, No. 1, 32–39, 2004.
10. Jun Yang, Zhili Zeng, Yufei Tang, Jun Yan, Haibo He, Yunliang Wu, Load frequency control in isolated micro-grid with electrical vehicle based on multivariable generalized predictive theory, Science World Journal, Vol.1, No.1, 2145-2164, 2015.
11. X. Sui, Y. Tang, H. He, J. Wen, Energy-storage-based low frequency oscillation damping control using particle swarm optimization and heuristic dynamic programming, IEEE Transaction on Power System, Vol. 29, No. 5, 2539-2548, 2014.
12. E. Yesil, Interval type-2 fuzzy PID load frequency controller using Big Bang–Big Crunch optimization,

Applied Soft Computing, Vol.15, 100–112, 2014.
13. M.H. Khooban, T. Niknam, A new intelligent online fuzzy tuning approach for multi-area load frequency control: self-adaptive modified bat algorithm, International Journal of Electric Power & Energy System, Vol. 71, No. 1, 254–261, 2015.
14. P. C. Sekhar and S. Mishra, Storage Free Smart Energy Management for Frequency Control in a Diesel-PV-Fuel Cell-Based Hybrid AC Microgrid, IEEE Trans. Neural Networks Learn. Syst., vol. 27, no. 8, 1657–1671, 2016.
15. P. Tielens and D. van Hertem, Grid Inertia and Frequency Control in Power Systems with High Penetration of Renewables, Proc. 6th IEEE Young Res. Symp. Electr. Power Eng., no. 2, pp. 1–6, 2012.
16. K. S. V. Phani Kumar and S. Venkateshwarlu, A Neuro-Fuzzy Controlled Solar Photovoltaic and PHEV based Frequency Regulation in a Microgrid without Storage System, J. Green Eng., vol. 7, no. 1, 311–332, 2017.
17. D. M. Robalino, G. Kumar, L. O. Uzoechi, U. C. Chukwu and S. M. Mahajan, Design of a docking station for solar charged electric and fuel cell vehicles, 2009 International Conference on Clean Electrical Power, Capri, 655-660, 2009
18. E. S. Rigas, S. D. Ramchurn, and N. Bassiliades, Managing Electric Vehicles in the Smart Grid Using Artificial Intelligence: A Survey, IEEE Trans. Intell. Transp. Syst., vol. 16, no. 4, 1619–1635, 2015.
19. S. Faddel, A. T. Al-Awami, and M. A. Abido, Fuzzy Optimization for the Operation of Electric Vehicle Parking Lots, Electr. Power Syst. Res., vol. 145, 166–174, 2017.
20. K. Mahmud and G. E. Town, A review of computer tools for modeling electric vehicle energy requirements and their impact on power distribution networks, Appl. Energy, vol. 172, pp. 337–359, 2016.
21. E. Kayacan and M. A. Khanesar, Fuzzy Neural Networks for Real Time Control Applications, BH Publications- Edition-1, 2017
22. NERC, Frequency Response Standard Background Document, 2012.

AUTHORS PROFILE

Phani Kumar K.S.V completed his B.Tech in Electrical and Electronics from Anna University and his M.E from S.R.M University Chennai. He is currently working for his Ph.D. in JNT University Hyderabad in the area of Distributed Generation, Optimization techniques and Power Quality, AI techniques. He is currently working as Assistant Professor in CVR College of Engineering, Hyderabad, Telangana, India.

Dr.S.Venkateshwarlu Completed his B.Tech from Sri Venkateshwara University, Tirupati in Electrical & Electronics Engineering, Masters from NIT Warangal with Electrical Machines & Industrial Drives specialization, Kakatiya University and Ph.D. from College of Engineering, Osmania University, Hyderabad in 2011. His areas of interests are Power Electronics, FACTS applications and Power quality. He is currently working as Professor & Head of EEE department at CVR College of Engineering, Hyderabad, Telangana, India.